Phosphorus-31 Nuclear Magnetic Resonance Study of Internal Motion in Ribonucleic Acid of Southern Bean Mosaic Virus†

Douglas C. McCain,‡ R. Virudachalam, Robert E. Santini, Sherin S. Abdel-Meguid,§ and John L. Markley*

ABSTRACT: Phosphorus-31 nuclear magnetic resonance spectroscopy was used to study southern bean mosaic virus (SBMV) in its native and ethylenediaminetetraacetic acid treated forms at various pH values in the range 4.5–9.0. The degree of swelling in the latter form is a critical function of pH. Spin–lattice relaxation time (T_1), line-width, and nuclear Overhauser effect (NOE) measurements were made at 40.51, 80.98, and 190.3 MHz. The results indicate that the RNA phosphate groups in native SBMV exhibit low-amplitude internal motions on a nanosecond time scale while the phosphate groups of swollen virus exhibit large-amplitude, more rapid, internal motions. A spread of T_1 and NOE values is measured at intermediate stages in the swelling process. A simple explanation, consistent with the data, is that the RNA core of the virus undergoes a two-state phase transition from a relatively rigid, compact solid form in the native SBMV to a mobile, solvated state in the fully swollen particle.

Southern bean mosaic virus (SBMV) particles have $T = 3$ (Caspar & Klug, 1962) icosahedral capsids with a weighted mean diameter of 285 Å (Johnson et al., 1976) and M_r of 6.6×10^6 (Lonberg-Holm & Korant, 1978). The particle consists of an RNA core encased by 180 identical protein molecules, each with M_r of 28 500. The complete amino acid sequence of the coat protein (260 residues) has been determined (Hermodson et al., 1982). In the X-ray structure, refined to 2.8-Å resolution (Abad-Zapatero et al., 1980), most of the viral coat appears as well-ordered structure. However, 43 residues in 60 subunits and 63 residues in 120 subunits at the amino terminus are randomly associated with the RNA. Many of these residues have basic side chains. Divalent cations play an important role in stabilizing SBMV (Hsu et al., 1976; Hull, 1978; Abdel-Meguid et al., 1981). Each virus particle sequesters approximately 180 Ca^{2+} and 180 Mg^{2+} ions (Abdel-Meguid et al., 1981). Cation removal with ethylenediaminetetraacetic acid (EDTA) at basic pH causes the virus to swell by about 7% in diameter (Rayment et al., 1979). Swollen virus particles shrink to about the diameter of native particles if the pH is lowered below 5.5 (Sehgal, 1980). McCain et al. (1982) used carbon-13 nuclear magnetic resonance (NMR) to show that a portion of the amino acid side chains exhibits much greater freedom of motion in swollen SBMV than in native SBMV. The coat protein of tomato bushy stunt virus (TBSV), which exhibits a protein fold similar to that of SBMV, also contains an amino-terminal arm, and the virus also swells on removal of cations (Harrison et al., 1978; Harrison, 1980). A common feature of the X-ray structures of SBMV and TBSV is the lack of resolution of the RNA components in the electron density maps (Harrison et al., 1978; Abad-Zapatero et al., 1980). The exterior part of the virus capsid has icosahedral symmetry, but the RNA and the flexible arm of the capsid are unlikely to have the same symmetry since there is only 1 RNA molecule per particle. Hence, the failure to resolve the RNA electron density may result from (1) lack of alignment of the RNA in identical crystalline virus particles (static disorder), (2) differences of rigid RNA organization within different virions (static disorder), and/or (3) constant internal motions within the virions (dynamic disorder).

^{31}P NMR relaxation measurements should provide information concerning the existence of rapid internal motions in the nucleic acid of virus particles (Bolton & James, 1979, 1980; Early & Kearns, 1979; Hogan & Jardetzky, 1979, 1980; Opella et al., 1980, 1981; Klevan et al., 1979; Shindo, 1980; Lipari & Szabo, 1981). On the basis of line-width analysis of ^{31}P NMR spectra of TBSV, Munowitz et al. (1980) concluded that the RNA of the native virus is highly immobile and that the observed lack of ordered electron density for either the RNA molecule or amino-terminal regions of the protein coat molecules of this virus (Harrison et al., 1978) results from static disorder. We report here longitudinal relaxation time (T_1), nuclear Overhauser effect (NOE), and line-width ($\Delta\nu_{1/2}$) data for native and EDTA-treated SBMV at various pH values in the range 4.5–9. These measurements indicate the presence of rapid motions for the RNA even of native SBMV that are incompatible with a highly static structure and suggest that this dynamic disorder could contribute to the lack of a defined X-ray pattern. In agreement with the results on TBSV (Munowitz et al., 1980), we find that the swelling of SBMV leads to increased mobility of the RNA. Our results indicate that a phase change occurs in the RNA structure as a result of swelling of the virus particle.

Experimental Procedures

Sample Preparation. Native SBMV (cowpea strain) was isolated by a modification (Johnson et al., 1974) of the procedure of Ghabrial et al. (1967). Metal-free SBMV was prepared from the native virus (Hsu et al., 1977) by dialysis against 0.04 M EDTA in 0.05 M phosphate buffer, pH 7.5. For ^{31}P NMR measurements the buffer was changed from phosphate to arsenate for both native and EDTA-treated samples by extensive dialysis against 0.25 M arsenate buffer, pH 7.0, and 0.05 M arsenate buffer, pH 7.5, respectively. The

† From the Purdue University Biochemistry Program and the Purdue University Biochemical Magnetic Resonance Laboratory, Purdue University, West Lafayette, Indiana 47907. *Received May 11, 1982.* This research was supported by National Institutes of Health Grant GM 19077 to J.L.M. and Postdoctoral Fellowship Grant 5 G32 GM7103 to S.S.A.-M. and National Science Foundation Grant PCM 78-16584 and NIH Grant AI 11219 to Michael G. Rossmann. NMR spectroscopy was carried out at the Purdue University Biochemical Magnetic Resonance Laboratory supported by NIH Grant RR01077 from the Biotechnology Resources Program of the Division of Research Resources.

‡ Present address: Department of Chemistry, University of Southern Mississippi, Hattiesburg, MS 39401.

§ Present address: Department of Molecular Biophysics and Biochemistry, Yale University, New Haven, CT 06511.

0006-2960/82/0421-5390$01.25/0

desired pH was achieved by dialysis against 0.05 M arsenate buffers of appropriate pH. Virus concentrations ranged from 9 to 28 mg mL^{-1}.

NMR Measurements. ^{31}P NMR spectra of SBMV were obtained at three different spectrometer frequencies. A Nicolet Technology Corp. NT-200 operating at a frequency of 80.98 MHz for ^{31}P was used for most of the work reported here. An NT-470 (190.3 MHz, 8-mm probe) and a modified Varian XL-100 (40.51 MHz, 12-mm probe) allowed us to study the effects of varying magnetic field strength. With the NT-200, 2.6-mL samples were placed in a spherical microcell (Wilmad Glass Co., Inc.) within a 20-mm tube. Standard NMR tubes (Wilmad) were used with the other instruments. All measurements were made at room temperature, 22 ± 2 °C. The spectrometers were not field locked since, for the broad lines observed, magnet drift is negligible over the period of observation.

T_1 measurements used the standard inversion–recovery pulse sequence $(180°-\tau-90°-\text{FID}-\text{PD})_x$ with x = 100–200. The pulse delay (PD) was varied from 14 to 80 s (usually 21 s), and 7–18 (typically 12) different τ values were used for each data set. For recovery of an NMR spectrum, the free induction decay (FID) was apodized, i.e., multiplied by some function of time such as an exponential, trapezoidal, or sinusoidal function, and then Fourier transformed. Apodization is normally used to reduce high-frequency noise, but it may also be used to emphasize or deemphasize lines according to their width. Multiplication by a sharply falling exponential adds a constant width to every line without changing its area and reduces the height of narrow lines more than it reduces that of wide lines. We measured T_1 in each data set after apodization by exponential line broadening parameters of 25, 50, 100, 200, 400, 800, and 1600 Hz, using from this list only those functions that gave an acceptable signal-to-noise ratio. In certain cases sinusoidal or trapezoidal apodization was used. The result was a set of T_1 values that appears to represent the relaxation time dispersion of ^{31}P nuclei in SBMV. Some data points were not plotted because of poor signal to noise. It is difficult to estimate error limits for these T_1 values since they represent weighted averages of a poorly defined distribution. If the T_1 were a single value, our measurements would be accurate to about ±20%, given the experimental signal-to-noise ratios. Better accuracy could be obtained only at the cost of impractically long spectrometer runs. Each T_1 set on the NT-200 or NT-470 required 11–18 h of instrument time; on the XL-100 each run lasted 2–3 weeks.

The apodized free induction decays were Fourier transformed and analyzed to obtain T_1 values by fitting peak heights or integrals to the function:

$$S(\tau) = S(\infty)(1 - [1 + W(1 - e^{-\text{PD}/T_1})]e^{-\tau/T_1}) \quad (1)$$

This function, included in the standard software supplied with Nicolet spectrometers, features a term (W) that compensates for the effects of pulse angle errors and inhomogeneous radio-frequency fields. Different T_1 data sets will typically achieve a least-squares fit to a nearly constant value of W characteristic of the particular spectrometer used. SBMV, however, is not a typical sample, and we found that the fitted value of W differs greatly from the expected value. This is because the ^{31}P nuclei in SBMV exhibit a distribution of relaxation times. While the original justification for the W term had nothing to do with relaxation dispersion (Levy & Peat, 1975), the extra parameter provides a fortuitous opportunity for a qualitative description of the distribution. Calculations using simulated T_1 data sets, based on assumed T_1 distributions and τ values similar to those in the experimental data sets, led us to the following conclusions: (1) A single relaxation time, or a narrow, symmetrical distribution of relaxation times, fits a W parameter equal to the expected value for a particular spectrometer (e.g., 0.7–0.8 on the NT-200 with 20-mm samples). (2) A distribution of generally long relaxation times, contaminated by a small fraction of considerably shorter relaxation times, decreases W. (3) Short relaxation times, mixed with a small fraction of much longer times, generally increase W.

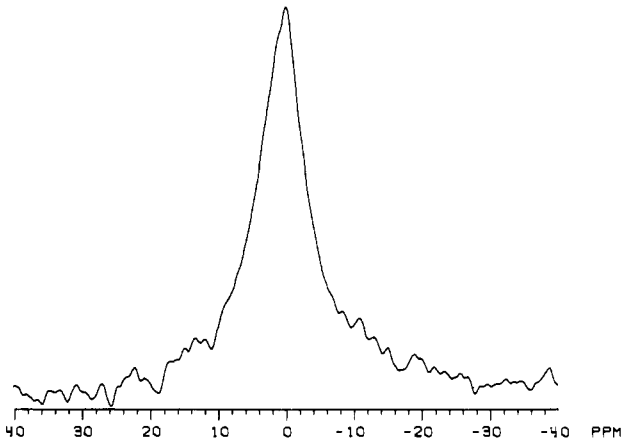

FIGURE 1: ^{31}P NMR spectrum at 80.98 MHz of native southern bean mosaic virus. About 20 mg mL^{-1} virus in 0.05 M arsenate buffer, pH 7.5, was placed in a spherical microcell within a 20-mm tube. Square wave modulated proton decoupling of 1.5 W was used. 90° pulses (32 μs) with delays of 21 s between pulses were averaged with 8K data points.

Proton-decoupled nuclear Overhauser effect (NOE) measurements on the NT-200 used the standard gated decoupling technique. NOE enhancement is defined as

$$\eta = \frac{S_{\text{on}} - S_{\text{off}}}{S_{\text{off}}} \quad (2)$$

where S_{on} and S_{off} are peak heights or integrals measured after a pulse delay of 21 s with the decoupler on or off, respectively. So that heating could be limited, decoupler power was set to just over the lowest level that gave a maximum η (1.5 W). For some of the samples η varied with apodization parameters, and more than one value was recorded. Accuracy is estimated to be ±0.2.

Line widths and intensities were recovered from T_1 and NOE data sets as well as from conventional one-pulse experiments. Line width, $\Delta\nu_{1/2}$, is defined as the full width at half-height. The value reported is the measured value less the line broadening resulting from apodization. Similar apodization parameters were used for all line-width measurements. Experimental line widths did not vary with decoupling power. Intensities were measured from the total integral over the region ±20 ppm from peak center; they were taken from spectra without NOE enhancement and were normalized for the concentration of virus and the number of pulses. Control of systematic errors is difficult in relative intensity measurements, but we estimate our results are accurate to ±20%.

Results

Line Shape and Line Width. A single, wide line is seen in the spectrum of every sample as shown in Figure 1 for native SBMV at pH 7.5. Figure 2 compares spectra of EDTA-treated SBMV at different pH values. Note that the line width decreases and that the line shape changes from triangular to approximately Lorentzian as the pH is increased from 4.5 to 9.0. Deconvolution by the use of different exponential apodization functions suggests that between pH 4.5 and pH 6.5

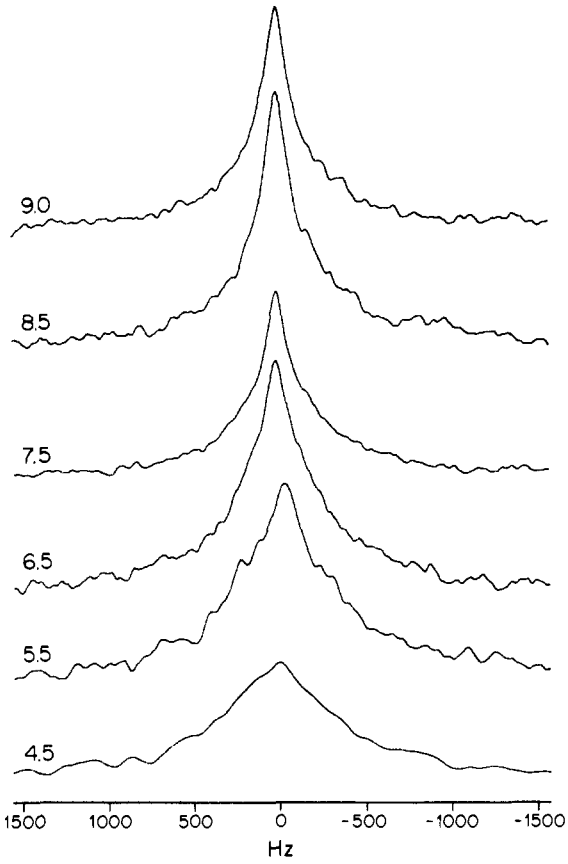

FIGURE 2: Comparison of ^{31}P NMR spectra at 80.98 MHz of EDTA-treated southern bean mosaic virus at various pH values. Experimental details are as described in Figure 1.

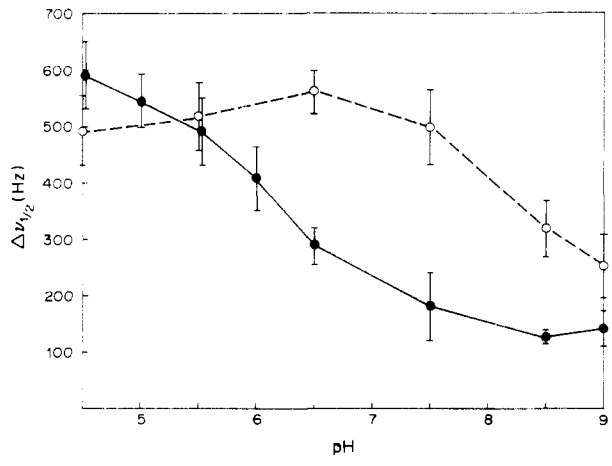

FIGURE 3: pH dependence of line width at half-height ($\Delta\nu_{1/2}$) of NMR peak of native southern bean mosaic virus (--) and EDTA-treated southern bean mosaic virus (—).

the spectrum is composed of overlapping lines with identical chemical shifts but with a distribution of different widths. We cannot resolve the spectrum into its individual lines, but we can estimate a characteristic spin–lattice relaxation time (T_1) associated with each range of line widths. Measured line widths at 80.98 MHz are shown in Figure 3. The line width, $\Delta\nu_{1/2}$, of EDTA-treated SBMV drops substantially above pH 5.5, while that of native SBMV remains nearly constant from pH 4.5 to pH 7 and decreases only above pH 7.5.

Integrated Intensities. Figure 4 presents relative integrated intensities from 12 samples; these values are independent of the apodization parameter used. The vertical scale, although arbitrary, is proportional to the NMR-detectable fraction of

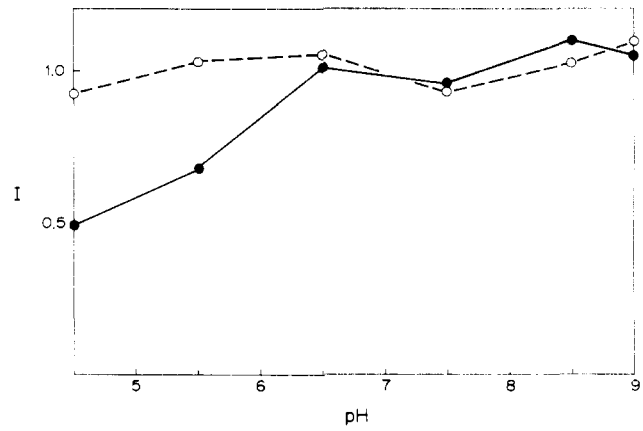

FIGURE 4: pH dependence of observed intensity (I) of ^{31}P NMR peak (relative to that of native virus at pH 6.5) of native southern bean mosaic virus (--) and EDTA-treated southern bean mosaic virus (—).

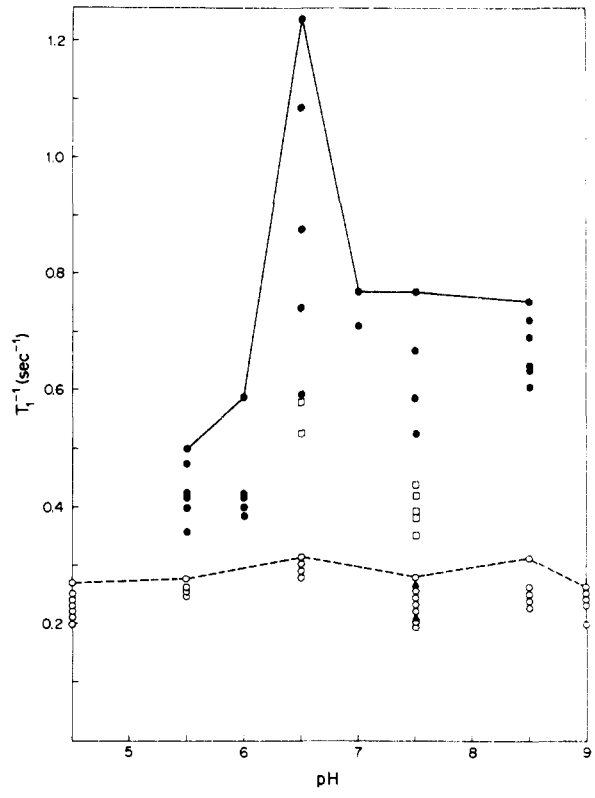

FIGURE 5: pH dependence of measured ^{31}P NMR longitudinal relaxation rate (T_1^{-1}) of components of the spectrum selected on the basis of line width. Relaxation measurements were made by using the standard inversion–recovery technique, but the raw free induction decays were apodized in turn by exponential line broadening parameters of 25, 50, 100, 200, 400, 800, and 1600 Hz (as described under Experimental Procedures) to investigate the possible dispersion of T_1 values associated with lines of different width that might be under the broad ^{31}P NMR peak. Native southern bean mosaic virus at 40.51 (▲) and 80.98 MHz (○); EDTA-treated southern bean mosaic virus at 40.51 (□) and 190.3 MHz (●). The line connects the T_1^{-1} values of the most rapidly relaxing components.

phosphorus nuclei in the virus. Results for native SBMV (dashed line) are independent of pH; evidently we see a constant fraction (probably 100%) of the nuclei. The same fraction is seen in swollen SBMV (solid line) from pH 6.5 to pH 9.0, but the intensity falls below pH 6.5. This decrease may be due to a phosphorus population with very long T_1 relaxation times that is unable to recover fully in the 21 s between pulses. It is unlikely to be due to excessively broad lines since rotational diffusion of the virus particle is fast

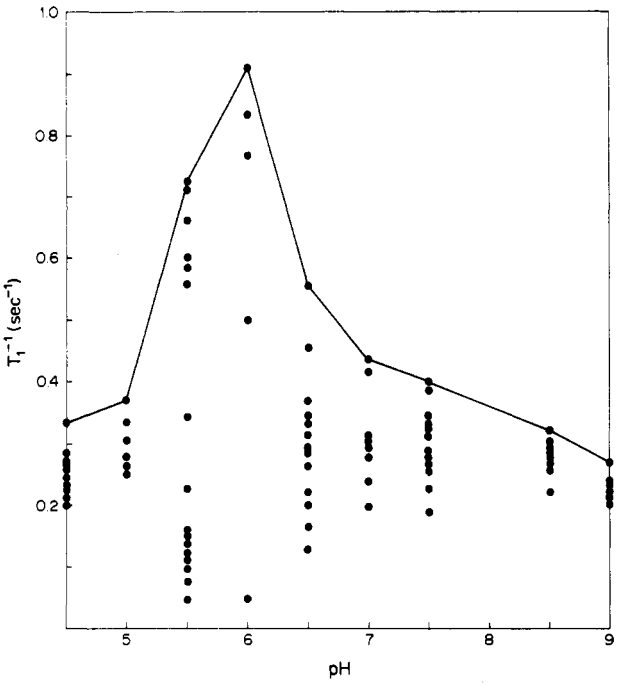

FIGURE 6: pH dependence of measured ^{31}P NMR longitudinal relaxation rate (T_1^{-1}) at 80.98 MHz of EDTA-treated southern bean mosaic virus. The data were analyzed as described in Figure 5. The line connects the T_1^{-1} values of the most rapidly relaxing components.

enough to narrow all RNA signals to approximately 700 Hz.

Relaxation Rates. Spin–lattice relaxation rates, T_1^{-1}, are displayed in Figures 5 (EDTA-treated virus at 190.3 and 40.51 MHz and native virus at 80.98 MHz) and 6 (EDTA-treated SBMV at 80.98 MHz). Each point in these figures represents a single T_1 determination. Each data set was reanalyzed a number of times with different apodization parameters (as described under Experimental Procedures) to reveal the range of T_1 dispersion associated with subspectral components having different line widths. In general, the uppermost points on the graph are the relaxation rates of the narrowest line components; other points are distributed downward approximately in order of increasing width. The lines on these figures connect the rates of the most rapidly relaxing fraction at each pH. The relaxation rates of native SBMV (Figure 5) are independent of pH and apodization parameter within experimental error. On the other hand, EDTA-treated SBMV (Figures 5 and 6) is dramatically different; between pH 5.5 and pH 6.5 the very large T_1^{-1} dispersion indicates a very heterogeneous assortment of phosphorus environments.

Line widths may be used to estimate low-frequency motions, but T_1 is more sensitive to high-frequency motions. Our T_1 data provide evidence for the existence of rapid internal motions in both native and swollen SBMV. Relaxation times as short as we observe can only be explained by invoking correlation times in the nanosecond range. This is far shorter than the 3-μs correlation time for reorientation of the entire virus particle.

The W Term. Figure 7 displays the average W terms obtained from T_1 data sets after a least-squares fit to eq 1 as described under Experimental Procedures. Error bars represent 1 standard deviation among the values recorded for different apodization parameters. A value of W between 0.7 and 0.8 would indicate a population of phosphorus nuclei with identical relaxation times or with a symmetrical distribution of short and long relaxation times. Data for native SBMV lie just slightly below the value expected for a uniform population. In EDTA-treated SBMV below pH 5.5, the data

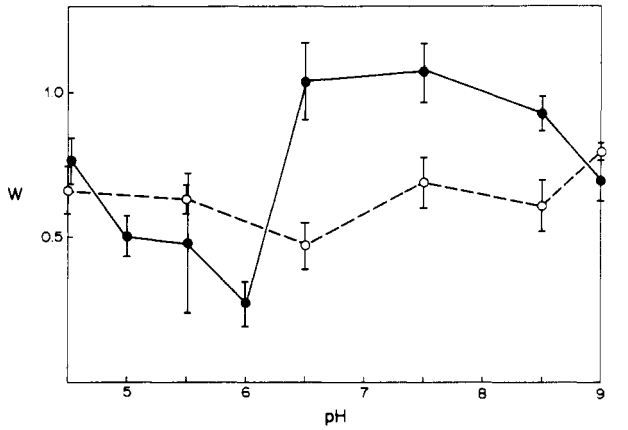

FIGURE 7: pH dependence of empirical factor W obtained from a three-parameter fit (Levy & Peat, 1975) of ^{31}P NMR T_1 relaxation data obtained at 80.98 MHz for native southern bean mosaic virus (– –) and EDTA-treated southern bean mosaic virus (—).

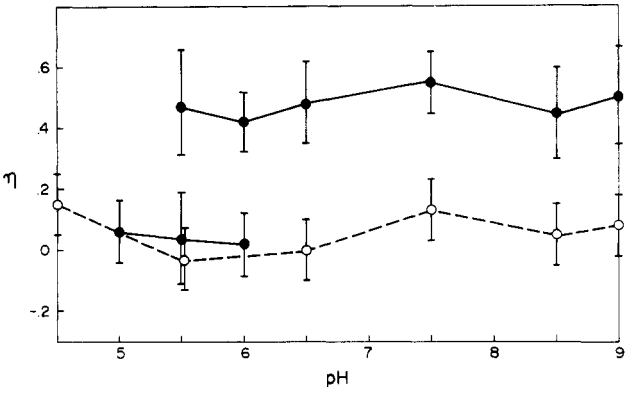

FIGURE 8: pH dependence of the nuclear Overhauser enhancement factor (η) determined for $^{31}P\{^1H\}$ NMR at 80.98 MHz of native southern bean mosaic virus (– –) and EDTA-treated southern bean mosaic virus (—).

correspond to a distribution of predominately long relaxation times with a small admixture of shorter times; above pH 6.0, T_1 is skewed in the opposite direction.

Nuclear Overhauser Effect. NOE data are shown in Figure 8. A nonzero η is direct evidence for relaxation by a $^1H\cdots^{31}P$ dipole–dipole mechanism with a relatively short correlation time. Within experimental error, the NOE of native SBMV is constant and nearly zero. This means that the dipole–dipole mechanism is not operative or that its correlation time is longer than 1 ns. The NOE of swollen SBMV above pH 7.5 is close to 0.5. In these samples dipole–dipole relaxation is important, and the correlation time is shorter than 1 ns. Between pH 5.5 and pH 6.5, the NOE of swollen SBMV is bimodal; apodization parameters favoring narrow lines give NOE values near 0.5, while wide lines have near zero NOE. Clearly the narrower lines belong to nuclei with more rapid correlation times.

Theory and Discussion

As stated above, our data provide evidence for internal motions at different rates in native and swollen SBMV. To interpret the data, we need an appropriate theory. Many theories of nuclear spin relaxation have been proposed; each has its merits and limitations. We have chosen to adapt the mathematically simple theory of Hogan & Jardetzky (1979, 1980) developed for double-helical DNA to RNA. This theory features a minimal number of adjustable parameters. Since motions in SBMV are undoubtedly more complex than the model assumes, our conclusions must be regarded as first approximations.

Line Widths. Our results may be compared with those of Munowitz et al. (1980), who obtained ^{31}P spectra of tomato bushy stunt virus (TBSV) in its native and swollen form. They studied line widths as a function of spectrometer frequency and temperature, in solution and in the solid state, and offered convincing evidence from line-width calculations that solution line widths in native TBSV are due mainly to chemical shift anisotropy modulated by isotropic tumbling of the virus particle. Calculation of the line width for SBMV, by adoption of the procedure used for TBSV, yields $\Delta\nu_{1/2} = 534 \pm 50$ Hz for native SBMV at 80.98 MHz and 22 °C. The excellent agreement between our measured value (520 ± 60 Hz) and this calculated value suggests that very similar relaxation mechanisms are responsible for line widths in native SBMV and TBSV.

EDTA-treated TBSV and EDTA-treated SBMV both swell as the pH is raised to neutrality, and their ^{31}P NMR peaks narrow. The reported line width for swollen TBSV at pH 7.0 is about 46% that of native TBSV. By comparison, the line width for swollen SBMV is 44% that of the native virus at pH 7.0 (interpolated). Again, the excellent agreement between swollen TBSV and swollen SBMV data is evidence that the RNA behaves similarly in both systems. Internal motion must be present in the swollen viruses, which effectively averages a large fraction of the chemical shift anisotropy.

Munowitz et al. (1980) considered only chemical shift anisotropy in their theoretical analysis of the line width of TBSV. We anticipate an additional contribution from the dipole–dipole mechanism. If one neglects the contribution from other mechanisms, such as magnet inhomogeneity (known to be very small) and variations in the isotropic chemical shift (for which we have no evidence, i.e., no line assymmetry), line widths may be calculated from

$$\Delta\nu_{1/2_{calcd}} = (\pi T_{2_{CS}})^{-1} + (\pi T_{2_{DD}})^{-1} \quad (3)$$

where $T_{2_{CS}}$ and $T_{2_{DD}}$ are the spin–spin relaxation times due solely to the chemical shift anisotropy and dipole–dipole mechanisms, respectively.

For rigid RNA within the virus particle, T_2 will be governed by the correlation time for isotropic rotational diffusion, τ_R, given by the Debye equation:

$$\tau_R = 4\pi\bar{\eta}r^3/(3kT) \quad (4)$$

At $T = 295$ K, by use of the viscosity of pure water ($\bar{\eta} = 0.01$ P) and the weighted mean radius of SBMV ($r = 142.5$ Å), eq 4 gives $\tau_R = 3$ μs. T_2 is also a function of ω_P, the angular precession frequency of the ^{31}P nuclei; $\omega_P = 2\pi\nu = 508.8 \times 10^6$ s^{-1} for the measurements in Figure 3. Since $\tau_R\omega_P \gg 1$, we can neglect several terms in the standard equations (Abragam, 1961) for T_2 and write approximately

$$T_{2_{DD}}^{-1} = (3/10)\gamma_H^2\gamma_P^2\hbar^2\tau_R\sum_i r_i^{-6} \quad (5)$$

$$T_{2_{CS}}^{-1} = (2/15)\omega_P^2\tau_R(\sigma'_x{}^2 + \sigma'_y{}^2 + \sigma'_z{}^2) \quad (6)$$

where γ_H and γ_P are the magnetogyric ratios of ^1H and ^{31}P, $\sum_i r_i^{-6}$ is a sum running over the internuclear distances (r_i) between the relaxing ^{31}P and all neighboring ^1H nuclei, and the σ' terms are the anisotropic part of the x, y, and z components of the chemical shift tensor. Assuming the σ' values reported for TBSV ($\sigma'_x = 79$ ppm, $\sigma'_y = 20$ ppm, $\sigma'_z = -99$ ppm), which are almost identical with those from other samples of RNA or DNA (Munowitz et al., 1980), and considering three protons at $r_i = 2.8$ Å from ^{31}P as in a typical DNA or RNA structure (Klevan et al., 1979; Hogan & Jardetzky, 1980), one can calculate the line width from eq 3–6. In SBMV we obtain $(\pi T_{2_{CS}})^{-1} = 534$ Hz, $(\pi T_{2_{DD}})^{-1} = 167$ Hz, and $\Delta\nu_{1/2} = 701$ Hz, which is larger than the measured line widths of $\Delta\nu_{1/2} = 520 \pm 60$ Hz in native SBMV or 150 ± 40 Hz for EDTA-treated SBMV above pH 7. This discrepancy indicates that internal motions need to considered.

The model developed by Hogan & Jardetzky (1979, 1980) to treat NMR relaxation times in short segments of helical DNA assumes rapid two-state fluctuations about the helical axis and slow rotational diffusion of the entire molecule. In SBMV the equivalent internal motion corresponds to fluctuation of a nucleotide unit about its phosphodiester bonds. Helical DNA behaves as a freely diffusing cylinder with two principal rotational correlation times, while rotation of the icosahedral SBMV particle is isotropic. Therefore, we can modify Hogan & Jardetzky's (1979) eq 1, replacing the two correlation times τ_L and τ_S by τ_R, the single rotational correlation time of a sphere. The result is

$$\Delta\nu_{1/2} = (1 - \beta)\Delta\nu_{1/2_{calcd}} \quad (7)$$

where β is a function of Δ, the amplitude of the fluctuation. For the special case of pure dipole–dipole relaxation, Hogan and Jardetzky give

$$\beta = (3/4)\sin^2\Delta \quad (8)$$

For SBMV, with its mixture of dipole–dipole and chemical shift anisotropy mechanisms, β is a more complex function [see Shindo (1980)], which could not be solved for Δ without detailed knowledge of the RNA conformation. We shall regard β as merely an indicator that shows the degree of freedom along the internal motion coordinates. Lipari & Szabo (1981) have critically reexamined the theory of Hogan and Jardetzky and found a mathematical error that has no effect on the equations used in this paper.

Using line-width data from native SBMV, we find $\beta = 1 - (520/700) = 0.26$. In EDTA-treated SBMV, β is 0.15, 0.22, 0.30, 0.42, 0.59, 0.74, 0.81, and 0.79 at pH 4.5, 5.0, 5.5, 6.0, 6.5, 7.5, 8.5, and 9.0, respectively. The uncertainty in β due to experimental error is approximately ±0.08 in each case, and β is not well-defined for swollen SBMV from pH 4.5 to pH 6.5 because the lines are non-Lorentzian. There may be an additional systematic error in β due to approximations in τ_R and r_i used to obtain $\Delta\nu_{1/2_{calcd}}$. Nevertheless, the change in β is very great, much greater than any reasonable range of error limits. Clearly β changes from a rather small number at low pH to a number near its theoretical limit (0.75 in eq 8) at high pH. We interpret these results to mean that restricted internal motion occurs in native SBMV and in EDTA-treated SBMV at low pH where the particle diameter is nearly the same as that in the native virus. However, internal motion of the RNA is essentially unrestricted in EDTA-treated SBMV above pH 7.

Hogan & Jardetzky (1980) applied their theory to internal motion in 140 and 260 base pair DNA fragments. They found rapid internal motion and $\beta = 0.5$. Lipari & Szabo (1981) attempted to compare the theory of Hogan and Jardetzky to a variety of theories describing models for internal motion. They concluded that all models considered predict large amplitude motion on a nanosecond time scale but that the data are too limited to allow identification of a unique "best" model. Others have examined DNA or RNA packaged in virus particles or in nucleosomes. Opella and co-workers (Opella et al., 1980; DiVerdi & Opella, 1981) found no evidence for internal motion within the filamentous bacteriophage fd. Evidence for internal motion was presented by Munowitz et al. (1980) for the RNA of swollen (but not native) TBSV, by Klevan et al. (1979) for nucleosome DNA, by Akutsu et al.

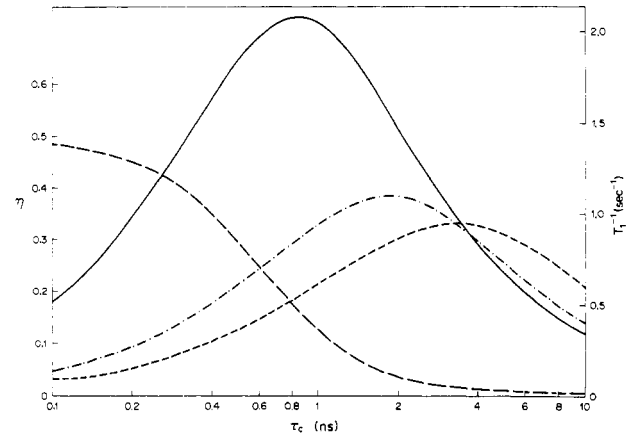

FIGURE 9: Dependence on correlation time of nuclear Overhauser enhancement (NOE) factor (η) at 80.98 MHz (– –) and of longitudinal relaxation rate (T_1^{-1}) at 40.51 (- - -), 80.98 (– · –), and 190.3 (—) MHz as calculated from eq 9 and 13.

(1980) for DNA of the bacteriophage PM2, and by Shindo et al. (1980) for nucleosome DNA.

Spin–Lattice Relaxation. Both dipole–dipole and chemical shift anisotropy mechanisms (Abragam, 1961) contribute to T_1 in SBMV.

$$T_{1_{calcd}}^{-1} = T_{1_{CS}}^{-1} + T_{1_{DD}}^{-1} \quad (9)$$

For isotropic rotational diffusion with a single correlation time, τ_c

$$T_{1_{CS}}^{-1} = (1/10)\omega_P^2(\sigma'_x{}^2 + \sigma'_y{}^2 + \sigma'_z{}^2)J(\omega_P) \quad (10)$$

$$T_{1_{DD}} = (1/20)\gamma_H^2\gamma_P^2\hbar^2\sum_i r_i^{-6}[J(\omega_H - \omega_P) + 3J(\omega_P) + 6J(\omega_H + \omega_P)] \quad (11)$$

where

$$J(\omega) = 2\tau_c(1 + \omega^2\tau_c^2)^{-1} \quad (12)$$

The nuclear Overhauser enhancement is given by

$$\eta = \frac{\gamma_H T_{1_{DD}}[6J(\omega_H + \omega_P) - J(\omega_H - \omega_P)]}{\gamma_P T_1[J(\omega_H - \omega_P) + 3J(\omega_P) + 6J(\omega_H + \omega_P)]} \quad (13)$$

If SBMV were internally rigid, we could equate τ_c with τ_R (eq 4). If one uses $\tau_c = \tau_R = 3$ μs, $\omega_P = 508.8 \times 10^6$ s^{-1}, and the σ' and r_i values used in the line-width analysis, eq 9–13 predict $T_1^{-1} = 1.4 \times 10^{-3}$ s^{-1} and $\eta = 0$. ^{31}P nuclei with such slow relaxation rates could not have been detected under our experimental conditions. Orders of magnitude faster correlation times (in the range 0.1–10 ns) are necessary to account for the observed relaxation rates.

Figure 9 presents eq 9–13 in graphic form. The nuclear Overhauser enhancement factor, η, was calculated for the experimental conditions used to obtain Figure 8 (ν_P = 80.98 MHz). A separate T_1^{-1} curve was calculated for each of our NMR spectrometers to match the different data sets in Figures 5 and 6. Note that the relaxation rates all peak at approximately $\tau_c = \omega_P^{-1}$.

Hogan & Jardetzky (1979, 1980) treated the effect of axial fluctuations on T_1 and $\Delta\nu_{1/2}$. If one neglects the very small contribution from isotropic rotation, their eq 2 (Hogan & Jardetzky, 1979) becomes

$$T_1^{-1} = \beta T_{1_{calcd}}^{-1} \quad (14)$$

where $T_{1_{calcd}}$ is the T_1 calculated from eq 9–12. T_1^{-1} is reduced by the same fractional factor, β, that reduces the line width.

Equation 5 of Hogan & Jardetzky (1980), which concerns the calculation of the nuclear Overhauser enhancement, contains an error; the terms $1 - (\alpha + \beta)$ in the numerator and denominator should be enclosed in brackets. With this correction, the approximation $\tau_P\omega_P^{-1} \gg 1$, and with inclusion of relaxation by chemical shift anisotropy not considered by Hogan and Jardetzky, their eq 5 reduces to our eq 13. This result shows that η may be calculated directly from the correlation time for internal motion without correction by the geometry terms α and β.

Internal Motion in Native SBMV. Our results (Figure 5) show that T_1 is independent of pH in native SBMV. At 80.98 MHz, by averaging all samples, $T_1^{-1} = 0.25 \pm 0.03$ s^{-1} and $\eta = 0.0 \pm 0.1$. We also measured T_1 for native SBMV (pH 7.5) at two different field strengths and found $T_1^{-1} = 0.24 \pm 0.05$ s^{-1} at 40.1 MHz and $T_1^{-1} = 0.47 \pm 0.07$ s^{-1} at 190.3 MHz. By use of eq 14 with the value of β determined from native SBMV line widths (β = 0.26), these results may be compared with the four curves in Figure 9. All data points agree simultaneously with the theoretical $T_{1_{calcd}}^{-1}$ and η only if 1.3 ns $< \tau_c <$ 2.0 ns. The best fit is found at τ_c = 1.6 ns. For example, at τ_c = 1.6 ns and 190.3 MHz, $T_{1_{calcd}}^{-1} = (T_1\beta)^{-1} = 0.47/0.26 = 1.8$ in good agreement with the upper curve in Figure 9.

Our data provide a simple description of the state of RNA in native SBMV. There is a fairly homogeneous population of ^{31}P nuclei subject to low-amplitude internal motion with a correlation time of about 1.6 ns.

Internal Motion in EDTA-Treated SBMV. The data from EDTA-treated SBMV are complex, with dispersions in T_1 and η, pH dependence of NMR parameters, and unusual integrals and W parameters to be explained. However, by applying the theory described above, we can make some immediate observations. The maximum in the experimental 80.98-MHz relaxation rate at pH 6 (Figure 6) can be identified with the corresponding maximum at τ_c = 2 ns on the theoretical 80.98-MHz curve (Figure 9). The theoretical 190.3-MHz experimental maximum at pH 6.5 (Figure 5) matches the maximum at 0.8 ns on the theoretical 190.3-MHz curve (Figure 9). For EDTA-treated SBMV at pH 8.5 or 9.0, line-width data give $\beta \simeq 0.80$ from which we derive $T_{1_{calcd}}^{-1} = 0.4$ s^{-1} and τ_c = 0.3 ns. The measured NOE (η = 0.5 at pH 8.5 and pH 9) matches that calculated for τ_c = 0.3 ns (η = 0.4) fairly well. Apparently by this simple analysis we have deduced the correlation times of an important fraction of the ^{31}P nuclei. As expected, τ_c decreases when EDTA-treated SBMV swells on increasing the pH above 7.

Our success with the partial analysis above suggests that we are on the right track; however, in order to explain all the data simultaneously, it is necessary to consider specific models for the RNA dynamics. We do not want a highly detailed model because the data do not warrant it. Three very simple models are examined in the following paragraphs.

Model 1 assumes an inhomogeneous population of ^{31}P nuclei, each of which has a characteristic correlation time. Correlation times follow a distribution function that shifts to emphasize shorter correlation times as the pH rises. This model provides a simple explanation for T_1 and η dispersions and for changes in W. Shindo (1980) has developed a related model using a mathematical function for the τ_c distribution. His model differs from model 1 by the assumption of a homogeneous population of nuclei, each nucleus subjected to the full range of correlation times; thus his model predicts a single relaxation time with no T_1 dispersion. Shindo et al. (1980) analyzed ^{31}P NMR data from DNA in nucleosomes using a variable parameter in the τ_c distribution function. Their curve of T^{-1} vs. τ_c is very broad [e.g., see Shindo (1980), Figure 4]

with a width at half-height spread more than 2 orders of magnitude about the central maximum in T_1^{-1}. A τ_c distribution function with a similar width would be necessary in order to explain our T_1^{-1} values that range from 0.91 to 0.05 at pH 6. This conclusion raises two arguments against model 1 as applied to our data. (1) The necessary τ_c distribution function must be so broad that we should not easily resolve the shift in the T_1^{-1} maximum vs. pH caused by a change in spectrometer frequency from 80.98 to 190.3 MHz; yet we do see the maxima easily resolved, one at pH 6.0 and the other at pH 6.5 (compare Figures 5 and 6). (2) At about pH 6 the population includes some ^{31}P nuclei that exhibit the highest possible relaxation rate (at $\tau_c = 2$ ns). For samples slightly different from pH 6, the τ_c distribution would shift, but other nuclei would have this maximum rate. Thus as pH varies, the T_1 distribution also changes; but the maximum rate measured should remain constant. We do not observe a constant maximum; rather T_1^{-1} goes through a pronounced peak as pH varies. For these reasons we reject model 1.

Model 2 assumes an inhomogeneous population of nuclei but lets the correlation time for internal motion be a simple function of pH; i.e., a single τ_c (or a narrow distribution) is associated with each pH. In order to explain the T_1 dispersions, we postulate a continuous distribution in β, each nucleus having its own characteristic value. To fit our T_1^{-1} results at pH 6, β must range from 0.04 to 0.75, or nearly the entire possible range from rigid to free internal rotation about the RNA axis. This model succeeds where model 1 fails; i.e., it predicts a narrow peak in relaxation rates. It fails, however, to explain the η dispersion. At or near the maximum in T_1^{-1} at 80.98 MHz, η should be nearly zero according to eq 13. We find a distribution with η as high as 0.5 at pH 6. We also consider it unlikely that β could vary this dramatically, implying great variation in local environments without concomitant variation in τ_c.

Model 3 assumes two distinct populations of ^{31}P nuclei, each with its own τ_c and β. Both τ_c and the relative numbers of nuclei in each group are functions of pH. Our measurements provide four types of evidence for this model. (1) The integrated intensity data (Figure 3) suggest that some ^{31}P nuclei are absent or underrepresented in the NMR signal from samples at pH 4.5 and pH 5.5, probably because their T_1 is excessively long; the nuclei that are detected at low pH have T_1 in the normal range. (2) The measured T_1^{-1} distribution appears to be bimodal; points cluster at the high and low pH extremes but not at intermediate pH values (Figure 5). (3) The *W* curve (Figure 8) is evidence for a varying population ratio with equal numbers of the two populations at about pH 6.25, the point where the *W* curve crosses the normal value. (4) η is distinctly bimodal at pH 5.5 and pH 6.0 with two quite different values measured (Figure 8).

Two populations of ^{31}P nuclei in SBMV could arise naturally if the RNA in the core undergoes a phase transition. A two-phase core is not unreasonable. EDTA-treated SBMV at high pH is swollen relative to native SBMV. If one assumes that the coat is 60-Å thick in native SBMV and that the volume of the coat protein remains constant, then a 7% increase in diameter corresponds to an approximate doubling in core volume. This extra volume must be occupied by water. So if native SBMV contains homogeneous, nearly-rigid RNA as our data suggest (see above), then swollen SBMV could contain both nearly rigid and dissolved RNA in equilibrium. The two populations of RNA would be expected to have different correlation times and different β values, and their relative amounts would depend on the water content of the core (a function of pH). The more rigid RNA would contribute the slow relaxation rate observed in our T_1^{-1} distribution while internally mobile (dissolved) RNA would account for the faster rates.

Model 3 predicts a narrow T_1^{-1} maximum as a function of pH (if τ_c and β for solid RNA do not vary rapidly with pH), but it apparently fails to explain the nuclear Overhauser enhancements. The high value of η at pH 6, the pH at which T_1^{-1} is maximal, provides direct evidence for a significant contribution to T_1 relaxation by a dipole–dipole mechanism having a short correlation time ($\tau_c << 1$ ns), yet this is inconsistent with the position of the T_1^{-1} peak, which implies $\tau_c = 2$ ns. The objection can be removed if we add the following additional assumption to model 3. Let the RNA in the aqueous solution phase be hydrogen bonded to adjacent water molecules. RNA phosphate groups will not be protonated in the pH range studied, but it is certainly expected that they will be hydrogen bonded. A P···H internuclear distance of ca. 2.4 Å is normal for phosphate–water hydrogen bonds (McCain & Markley, 1980). At this distance the dipole–dipole interaction is strong, and the relaxation rate would be quite large except that in phosphate solutions hydrogen-bonded protons exchange very rapidly with bulk solvent. The exchange time is 11 ps in aqueous $H_2PO_4^-$ (McCain & Markley, 1980). This rapid exchange swamps out the rotational correlation mechanism, and the effective τ_c becomes the exchange time. If $\tau_c \simeq 11$ ps, the additional relaxation rate due to hydrogen-bonded protons would be too small to detect in our experiments. But exchange might be much slower in the viscous, crowded environment of the RNA solution phase within the swollen virus. If exchange correlation times were approximately 100 ps, they would add only a small amount to T_1^{-1} but would be sufficient to explain the NOE measurement ($\eta = 0.5$).

It is necessary to comment on an apparent discrepancy between "solid" RNA in native SBMV and "solid" RNA in EDTA-treated SBMV. T_1 in native SBMV is ca. 3 s at 80.98 MHz whereas in the more rigid phase of EDTA-treated SBMV, T_1 is about 20 s at pH 5.5. Extensive dialysis against EDTA removes calcium and magnesium ions from virus particles. Although the location of magnesium ions in SBMV virions is not known, two-thirds of the calcium ions was shown (Abdel-Meguid et al., 1981) to be on the protein–RNA interface. It is possible that a number of magnesium ions are also located on the protein–nucleic acid interface. After removal of these ions, magnesium ions may be replaced by sodium. Thus, the RNA core in EDTA-treated SBMV may be altered as a result and need not display identical internal motions.

Conclusions

We have obtained ^{31}P NMR line-width, T_1, and NOE data for RNA in SBMV as a function of pH and magnetic field strength. Our results comprise the largest set of NMR data ever obtained for a large protein–nucleic acid system. However, even this large data set is inadequate to justify the development of a satisfactory theory to describe RNA dynamics within the virus particle. A few observations can be made through analysis of the results by simple models.

The RNA within native SBMV undergoes rapid but restricted motions. If the RNA tertiary structure were rigid in each virion, the ^{31}P line width would have been 35% greater than that observed, and T_1 values would have been orders of magnitude greater than those measured. Analysis of the T_1 relaxation data suggests that ^{31}P nuclei in the native virus comprise a fairly homogeneous population having low-am-

plitude internal motions with a correlation time between 1 and 2 ns. T_1 relaxation provides clearer evidence for the existence of these motions than line-shape analysis. It would be of interest to measure T_1 values for TBSV to test the conclusions of Munowitz et al. (1980) based on line shape that the RNA of the native virus is rigid.

The RNA of swollen SBMV, like that of swollen TBSV (Munowitz et al., 1980), has highly mobile components with large amplitude motions. Our data are consistent with a two-state phase transition of the RNA from a relatively rigid, poorly solvated state in native SBMV to a mobile, highly solvated state in swollen SBMV. ^{31}P NMR provides a convenient method for studying this process.

Other questions about virus structure and dynamics may be answerable by ^{31}P NMR studies. Preliminary ^{31}P NMR results with belladonna mottle virus (BDMV) show that changes in pH have a dramatic effect on the mobility of RNA, even in its native form (R. Virudachalam, K. L. Heuss, P. Argos, and J. L. Markley, unpublished results). BDMV lies at the low end whereas SBMV and TBSV lie near the middle of the Kaper scale, which measures the strength of protein–nucleic acid interactions in viruses (Kaper, 1975).

Acknowledgments

We thank Michael G. Rossmann for suggestions and illuminating discussions and Jeanne M. Renzetti for assistance in preparing the manuscript.

References

Abad-Zapatero, C., Abdel-Meguid, S. S., Johnson, J. E., Leslie, A. G. W., Rayment, I., Rossmann, M. G., Suck, D., & Tsukihara, T. (1980) *Nature (London) 286*, 33–39.

Abdel-Meguid, S. S., Yamane, T., Fukuyama, K., & Rossmann, M. G. (1981) *Virology 114*, 81–85.

Abragam, A. (1961) *The Principles of Nuclear Magnetism*, Oxford Press, London.

Akutsu, H., Satake, H., & Franklin, R. M. (1980) *Biochemistry 19*, 5264–5270.

Bolton, P. H., & James, T. L. (1979) *J. Phys. Chem. 83*, 3359–3366.

Bolton, P. H., & James, T. L. (1980) *J. Am. Chem. Soc. 102*, 25–31.

Caspar, D. L. D., & Klug, A. (1962) *Cold Spring Harbor Symp. Quant. Biol. 27*, 1–24.

Diverdi, J. A., & Opella, S. J. (1981) *Biochemistry 20*, 280–284.

Early, T. A., & Kearns, D. R. (1979) *Proc. Natl. Acad. Sci. U.S.A. 76*, 4165–4169.

Ghabrial, S. A., Shepherd, R. J., & Grogan, R. G. (1967) *Virology 33*, 17–25.

Harrison, S. C. (1980) *Biophys. J. 32*, 139–153.

Harrison, S. C., Olson, A. J., Schutt, C. E., Winkler, F. K., & Bricogne, G. (1978) *Nature (London) 276*, 368–373.

Hermodson, M. A., Abad-Zapatero, C., Abdel-Meguid, S. S., Pudnak, S., Rossmann, M. G., & Tremaine, J. H. (1982) *Virology 119*, 133–149.

Hogan, M. E., & Jardetzky, O. (1979) *Proc. Natl. Acad. Sci. U.S.A. 76*, 6341–6345.

Hogan, M. E., & Jardetzky, O (1980) *Biochemistry 19*, 3460–3468.

Hsu, C. H., Sehgal, O. P., & Pickett, E. E. (1976) *Virology 69*, 587–595.

Hsu, C. H., White, J. A., & Sehgal, O. P. (1977) *Virology 81*, 471–475.

Hull, R. (1978) *Virology 89*, 418–422.

Johnson, J. E., Rossmann, M. G., Smiley, I. E., & Wagner, M. A. (1974) *J. Ultrastruct. Res. 46*, 441–451.

Johnson, J. E., Akimoto, T., Suck, D., Rayment, I., & Rossmann, M. G. (1976) *Virology 75*, 394–400.

Kaper, J. M. (1975) *The Chemical Basis of Virus Structure, Dissociation and Reassembly*, American Elsevier/North-Holland, New York.

Klevan, L., Armitage, I. M., & Crothers, D. M. (1979) *Nucleic Acids Res. 6*, 1607–1616.

Levy, G. C., & Peat, I. R. (1975) *J. Magn. Reson. 18*, 500–521.

Lipari, G., & Szabo, A. (1981) *Biochemistry 20*, 6250–6256.

Lonberg-Holm, K., & Korant, B. D. (1978) *Acta Crystallogr., Sect. B B34*, 575–576.

McCain, D. C., & Markley, J. L. (1980) *J. Am. Chem. Soc. 102*, 5559–5565.

McCain, D. C., Virudachalam, R., Markley, J. L., Abdel-Meguid, S. S., & Rossmann, M. G. (1982) *Virology 117*, 501–503.

Munowitz, M. G., Dobson, C. M., Griffin, R. G., & Harrison, S. C. (1980) *J. Mol. Biol. 141*, 327–333.

Opella, S. J., Cross, T. A., DiVerdi, J. A., & Sturm, C. F. (1980) *Biophys. J. 32*, 531–548.

Opella, S. J., Wise, W. B., & DiVerdi, J. A. (1981) *Biochemistry 20*, 284–290.

Rayment, I., Johnson, J. E., & Rossmann, M. G. (1979) *J. Biol. Chem. 254*, 5243–5245.

Sehgal, O. P. (1980) *Phytopathology 70*, 342–348.

Shindo, H. (1980) *Biopolymers 19*, 509–522.

Shindo, H., McGhee, J. D., & Cohen, J. S. (1980) *Biopolymers 19*, 523–537.